Electronic Supplementary Information

Heterointerface synergy between 3×3 tunnel τ-MnO_2 cathode and $Mg_2(OH)_3Cl·4H_2O$ achieving long-cycle life for aqueous zinc-ion battery

Fang Xu[a], Jialin Zheng[a], Dai-Huo Liu[a,b,*], Ao Wang[a], Zhenjiang Li[a], Chunyan Xu[a], Mengqin Song[a], Beinuo Zhang[a], Zhengyu Bai[a,*] and Zhongwei Chen[b,*]

[a] Key Laboratory of Green Chemical Media and Reactions, Ministry of Education Collaborative Innovation Center of Henan Province for Green Manufacturing of Fine Chemicals, School of Chemistry and Chemical Engineering, Henan Normal University Xinxiang 453007, Henan, P. R. China.

[b] State Key Laboratory of Catalysis, Power Battery & Systems Research Center, Dalian Institute of Chemical Physics, Chinese Academy of Sciences, Dalian,110623, China.

Corresponding Authors: *E-mail: liudaihuo@htu.edu.cn, baizhengyu@htu.edu.cn, zwchen@dicp.ac.cn.

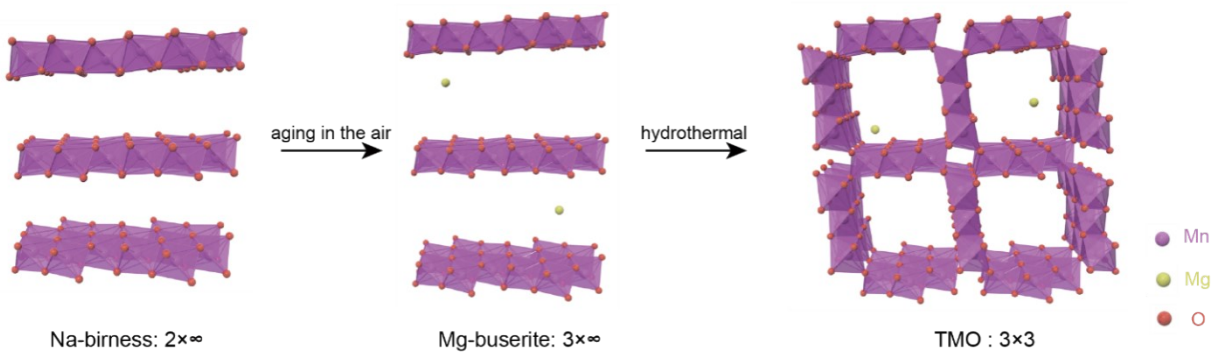

Fig. S1. Schematic illustration of the structural changes of TMO during preparation.

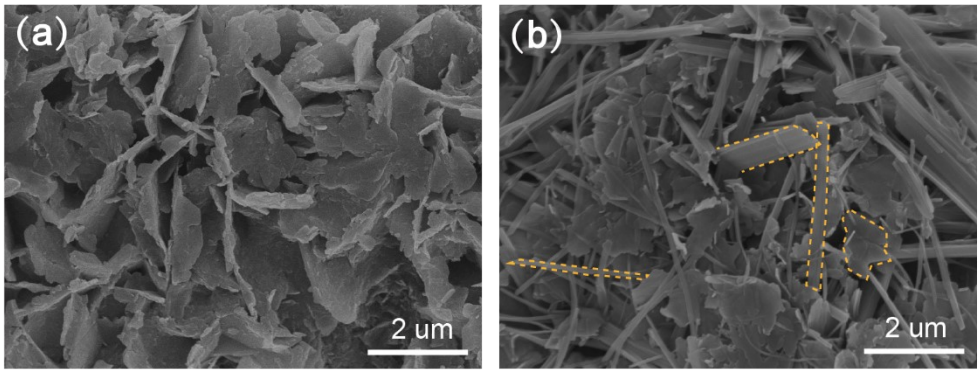

Fig. S2. SEM images of a) TMO-MOC heterostructure and b) TMO samples.

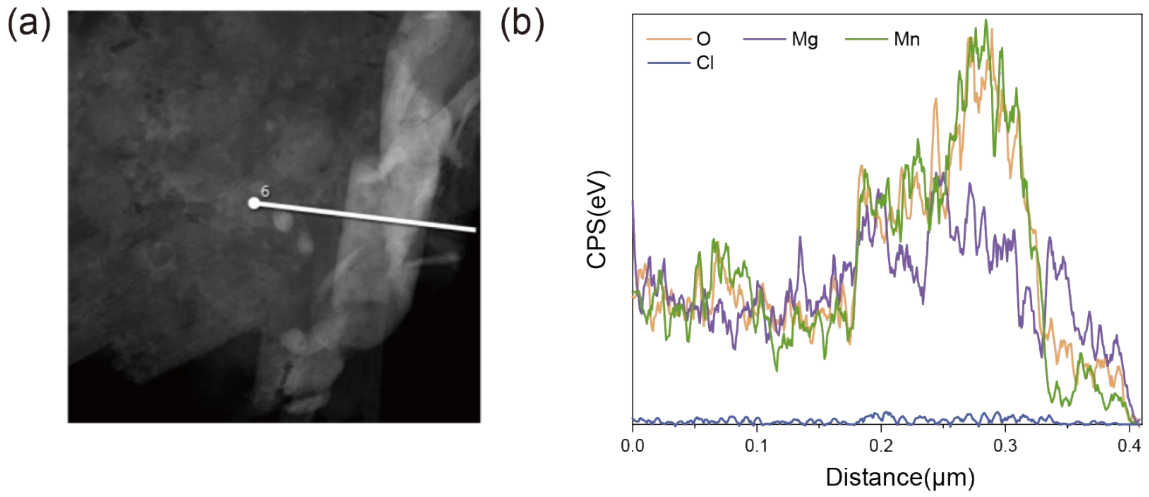

Fig. S3. (a) and (b) show the energy dispersive spectroscopy (EDS) of TMO-MOC heterostructure.

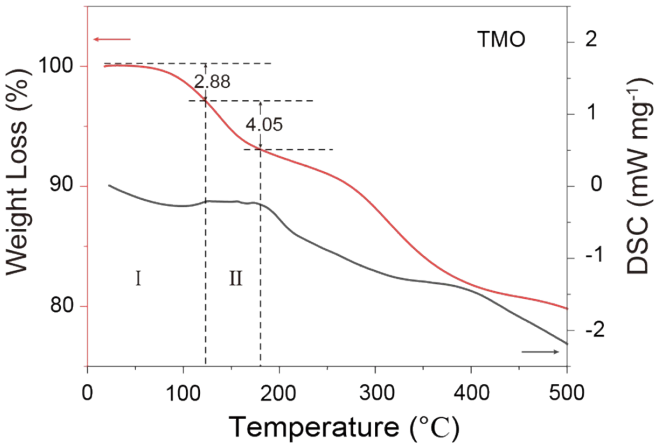

Fig. S4. TGA of TMO.

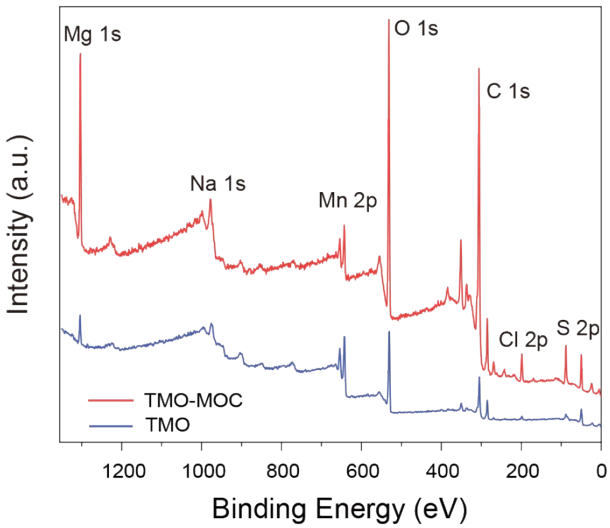

Fig. S5. XPS spectra of TMO-MOC heterostructure and TMO.

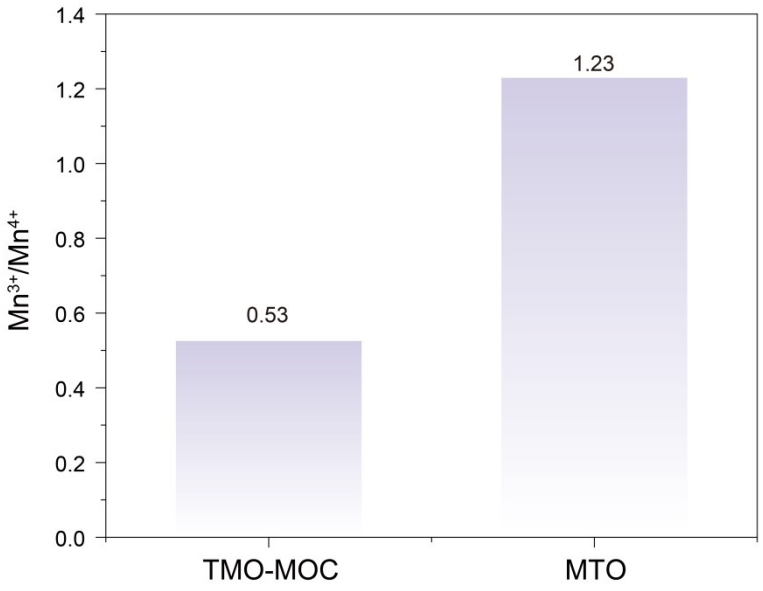

Fig. S6. The ratio of Mn^{3+}/Mn^{4+} in TMO-MOC heterostructure and TMO.

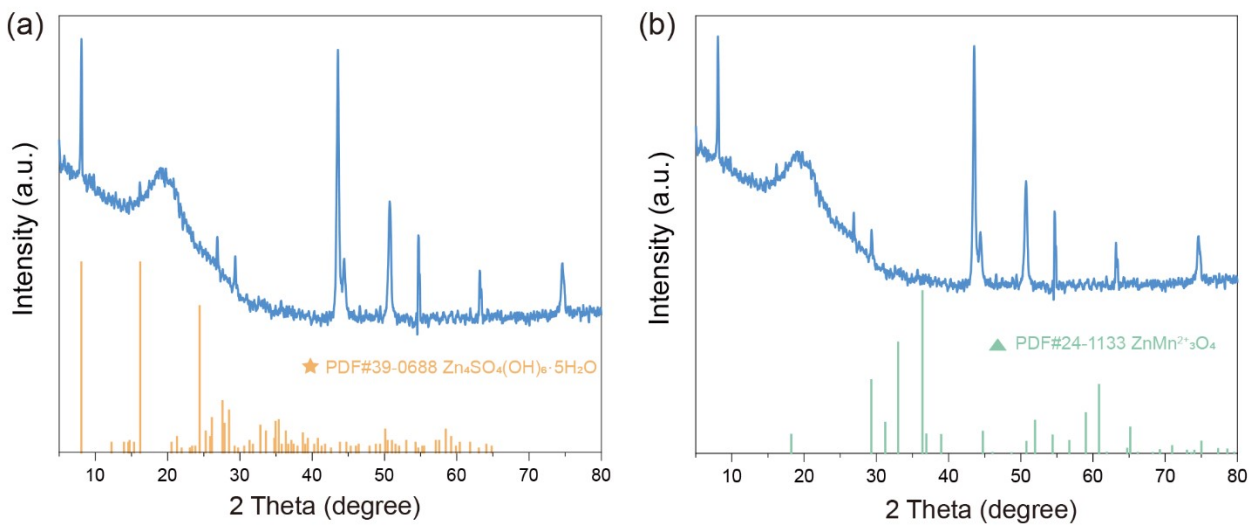

Fig. S7. (a,b) XRD of TMO-MOC heterostructure upon dischaging to 0.9V.

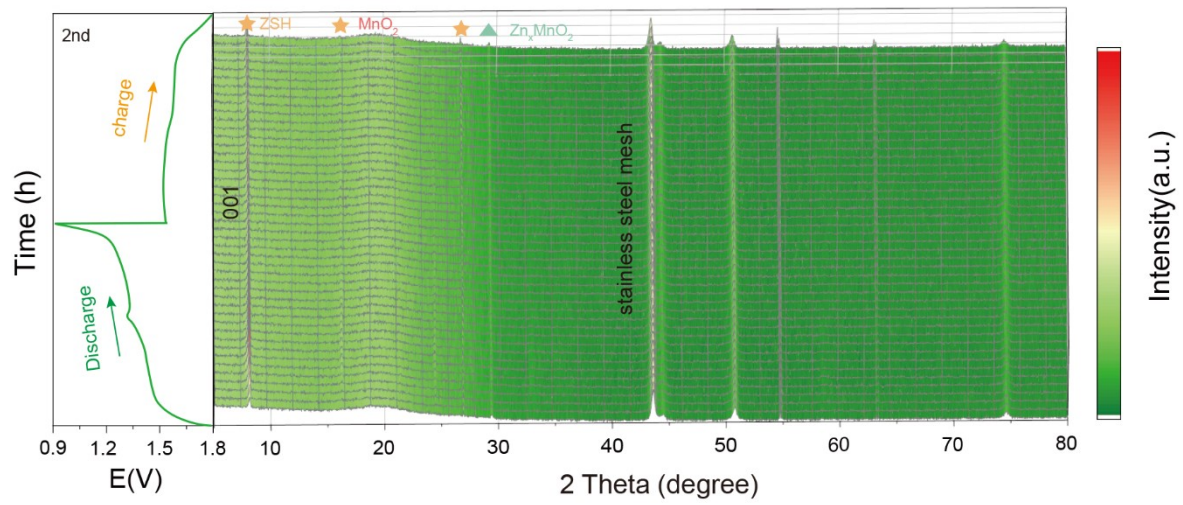

Fig. S8. *In-situ* XRD patterns in different discharge/charge states at 0.1 A g^{-1} of TMO-MOC heterostructure.

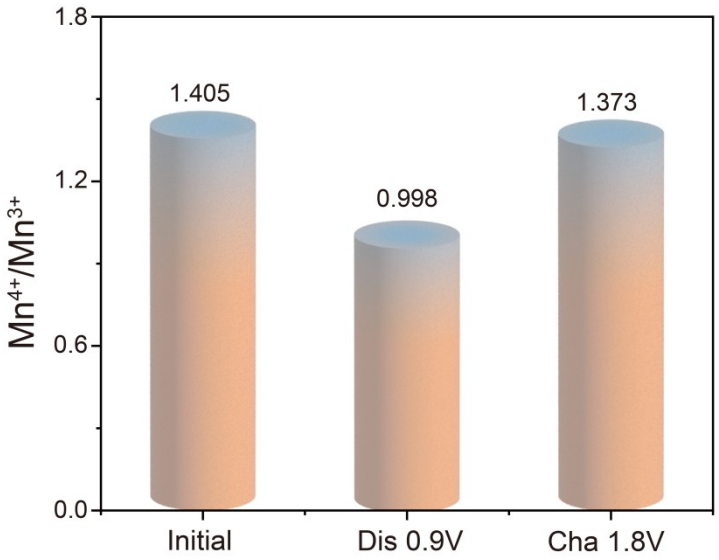

Fig. S9. The ratio of Mn^{4+}/Mn^{3+} in TMO-MOC heterostructure in different discharge/charge states.

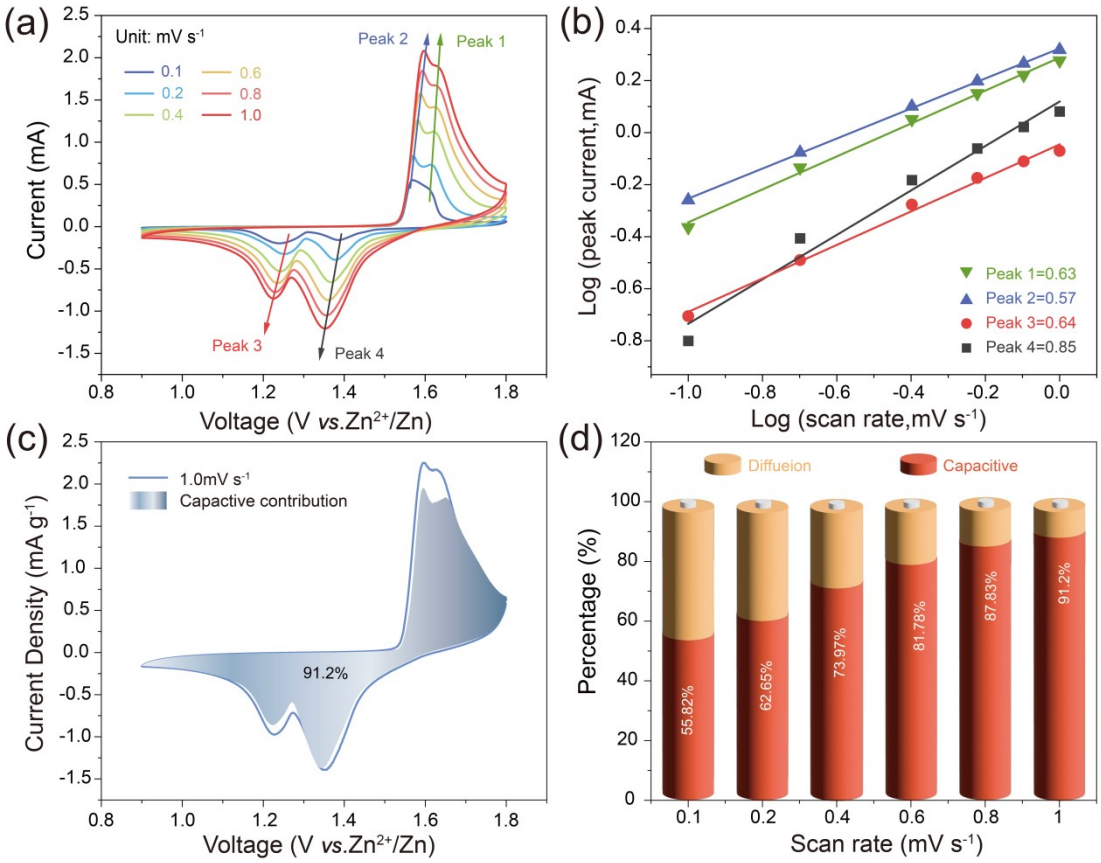

Fig. S10. Kinetics analyses of the electrochemical reactions in TMO. a) CV curves of the various scan rates, b) log(i) versus log(v) plots at different oxidation and reduction states, c) CV curve and pseudo capacitance contribution ratio at 1 mV s^{-1} scanning speed, d) The ratio of capacitive contribution at different scan rate.

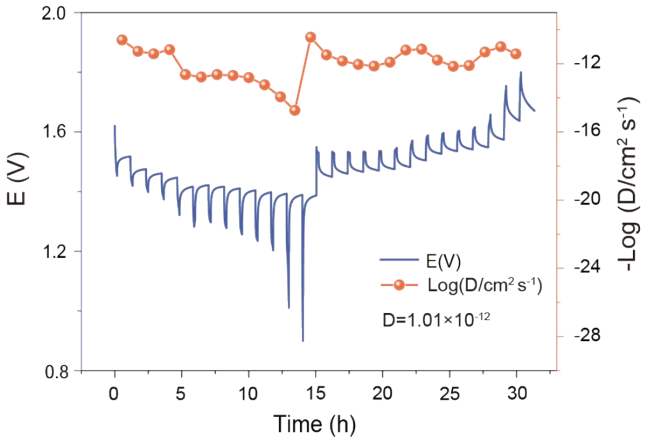

Fig. S11. GITT curve of TMO.

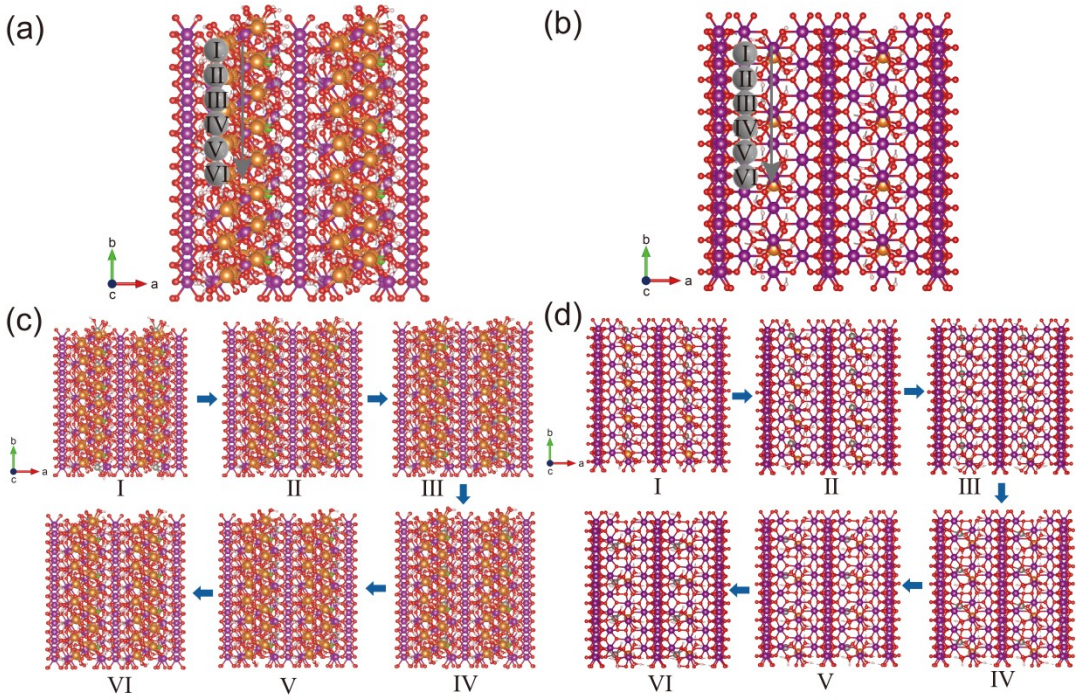

Fig. S12. Zn^{2+} diffusion pathway after projection (a) in TMO-MOC and (b) in TMO. The genuine diffusion pathway of Zn^{2+} (c) in TMO-MOC and (d) in TMO.

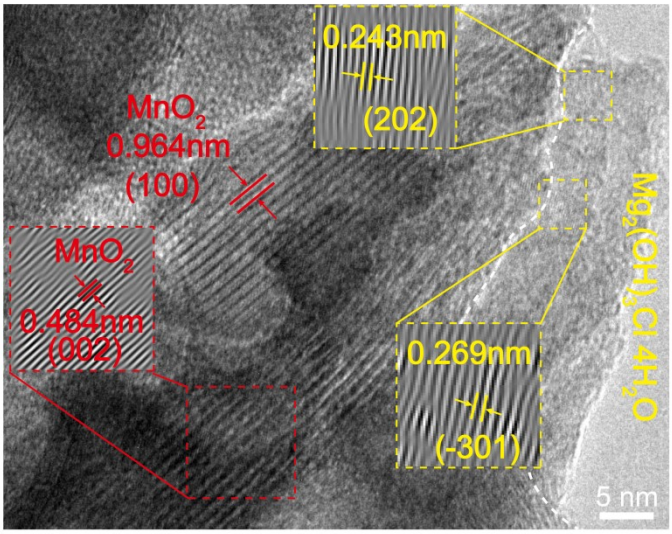

Fig. S13 . HRTEM of TMO-MOC heterostructure after 600 cycles.

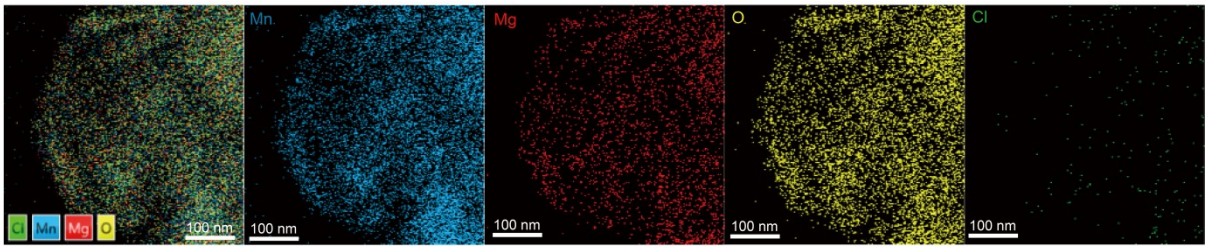

Fig. S14 . TEM elemental mapping of TMO-MOC heterostructure after 600 cycles.

Table S1. ICP-AES of TMO-MOC heterostructure and TMO.

	TMO-MOC	TMO
Mn(mg/L)	1	1
Mg(mg/L)	2.38	0.38

Table S2. XPS data of TMO-MOC heterostructure.

Name	start BE	Peak position BE	end BE	height CPS	FWHM eV
Mg1s	1315.07	1303.31	1295.17	77440.79	2.23
Mn2p	665.03	642.41	630.23	13640.94	2.73
O1s	545.07	531.25	525.17	91664.8	1.9
C1s	295.07	284.8	275.17	17164.18	1.49
Cl2p	210.07	198.36	190.17	8172.4	2.62

Table S3. XPS data of TMO.

Name	start BE	Peak position BE	end BE	height CPS	FWHM eV
Mg1s	1315.35	1304.04	1295.45	18271.85	1.93
Mn2p	665.31	642.19	630.51	23114.55	2.99
O1s	545.35	529.96	525.45	34004.29	2.74
C1s	295.35	284.8	275.45	9297.49	1.57
Cl2p	210.35	198.05	190.45	1916.76	1.74

Table S4. The electrochemical performances of TMO-MOC compared with other reported MnO_x cathodes in AZIBs.

Materials	First Cycle Capacity ($mAh\ g^{-1}$)	Cycle Numbers [at $1A\ g^{-1}$]	References
TMO-MOC	260 $mAh\ g^{-1}$ at $0.1A\ g^{-1}$	1800	This work
Mn_2O_3@$ZnMn_2O_4$/C	183.8 $mAh\ g^{-1}$ at $0.2A\ g^{-1}$	700	[1]
MnO_2	275 $mAh\ g^{-1}$ at $0.3\ A\ g^{-1}$	500	[2]
$Al_{0.1}$–MnO_2	347.6 $mAh\ g^{-1}$ at $0.1\ A\ g^{-1}$	1000	[3]
Cu-MnO_2	443 $mAh\ g^{-1}$ at $0.1A\ g^{-1}$	175	[4]
δ-MnO_2 NDs	335 $mAh\ g^{-1}$ at $0.1A\ g^{-1}$	1000	[5]
MO-s	392 $mAh\ g^{-1}$ at $0.5A\ g^{-1}$	1000	[6]
KMO	231.97 $mAh\ g^{-1}$ at $0.1A\ g^{-1}$	1400	[7]
Al – MnO	345 $mAh\ g^{-1}$ at $0.1A\ g^{-1}$	500	[8]
$Ag_{0.4}Mn_8O_{16}$	306 $mAh\ g^{-1}$ at $0.1A\ g^{-1}$	800	[9]
Mo-MnO_2	327 $mAh\ g^{-1}$ at $0.2A\ g^{-1}$	1000	[10]
ZNCMO@N-rGO	204.4 $mAh\ g^{-1}$ at $0.01A\ g^{-1}$	900	[11]
V_O-MnO_2@CNFs	268 $mAh\ g^{-1}$ at $0.05A\ g^{-1}$	740	[12]

References

1. Z. Gao, G. g. Lu, L. c. Cao, Z. x. Zhu, Y. x. Li, F. x. Wei, Z. Ji, Y. w. Sui, J. q. Qi, Q. k. Meng and Y. j. Ren, Rationally designed Mn_2O_3@$ZnMn_2O_4$/C core–shell hollow microspheres for aqueous zinc-ion batteries, *Dalton Trans.*, 2023, **52**, 1768-1776.
2. J. Wang, J. G. Wang, H. Liu, C. Wei and F. Kang, Zinc ion stabilized MnO_2 nanospheres for high capacity and long lifespan aqueous zinc-ion batteries, *J. Mater. Chem. A*, 2019, **7**, 13727-13735.
3. Y. Zhao, S. Zhang, Y. Zhang, J. Liang, L. Ren, H. J. Fan, W. Liu and X. Sun, Vacancy-rich Al-doped MnO_2 cathodes break the trade-off between kinetics and stability for high-performance aqueous Zn-ion batteries, *Energy Environ. Sci.*, 2024, **17**, 1279-1290.
4. J. Zhang, W. Li, J. Wang, X. Pu, G. Zhang, S. Wang, N. Wang and X. Li, Engineering p-Band Center of Oxygen Boosting H^+ Intercalation in δ-MnO_2 for Aqueous Zinc Ion Batteries, *Angew. Chem. Int. Ed.*, 2023, **62**.
5. H. Tang, W. Chen, N. Li, Z. Hu, L. Xiao, Y. Xie, L. Xi, L. Ni and Y. Zhu, Layered MnO_2 nanodots as high-rate and stable cathode materials for aqueous zinc-ion storage, *Energy Storage Mater.*, 2022, **48**, 335-343.
6. Y. Liu, J. Yao, J. Jiang, Y. Li and Q. Zhu, Exploring the effect of different additives on the preparation of α-Mn_2O_3/Mn_3O_4 composites and their zinc ion storage performances, *Ionics*, 2023, **29**, 1469-1478.
7. Q. Yang, Y. Chen, Y. Yang, T. Xu, Y. Lin, X. Zhang, J. Wang, Y.-N. Liu and Y. Li, Batch Synthesis of K-Doped α-MnO2 Nanorods as Cathode Materials for Aqueous Zinc-Ion Battery, *Ind. Eng. Chem. Res.*, 2023, **62**, 16757-16765.
8. Bo He, Jing Huang, Peng J, Tuan K.A. Hoang, Mei Han, Linjie Li, Lei Zhang, Zhongfeng Gao, Junhong Ma, Jian Zhi, P. Chen, Al doped manganous oxide for high-performance aqueous Zn-ion batteries, *J. Power Sources*, 2023, **554**.
9. B. W. O. Fekadu Wubatu Fenta, Meng-Che Tsai, Nigusu Tiruneh Temesgen, Wei-Hsiang Huang, Teshager Mekonnen Tekalign, Yosef Nikodimo, She-huang Wu, Wei-Nien Su, Hongjie Dai, Bing Joe Hwang, Structural engineering of α-MnO_2 cathode by Ag^+ incorporation for high capacity aqueous zinc-ion batteries, *J. Power Sources*, 2022, **548**, 232010
10. K. H. Zhen Wang, Qi Wan, Yixing Fang, Xuanhui Qu, and Ping Li, Mo-Pre-Intercalated MnO_2 Cathode with Highly Stable Layered Structure and Expanded Interlayer Spacing for Aqueous Zn-Ion Batteries, *ACS Appl. Mater. Interfaces*, 2023, 859−869
11. Z. L. Yayuan Tao, Linbin Tang, Xiaoming Pu, Tong Cao, Danhong Cheng, and H. L. Qunjie Xu, YongGang Wan, Yongyao Xia, Nickel and cobalt Co-substituted spinel $ZnMn_2O_4$@N-rGO for increased capacity and stability as a cathode material for rechargeable aqueous zinc-ion battery, *Electrochim. Acta*, 2020, **331**, 2020.
12. Q. S. Wei Liu, Rongrong Zhu, Weihao Shi, Fang Zhang, Gaohui Du, Wenqi Zhao, Miao Zhang, and Bingshe Xu, Chemical Lithiation-Induced Oxygen Vacancies in MnO_2 at Room Temperature for Aqueous Zinc-Ion Batteries, *ACS Appl. Energy Mater.*, 2023, 6689−6699.